DEM-BASED MODELING AND CONTACT PARAMETER CALIBRATION OF HAZELNUTS
/
基于 DEM 榛子建模与接触参数标定

Chun WANG[1)], Hailin KUI[1)], Xiaoli WU[1)], Yongchao SHAO[2)], Minggang FU[*1)]
[1)]College of Biological and Agricultural Engineering, Jilin University, Changchun 130000, China;
[2)]College of Mechanical Electrical Engineering, Northwest A&F University, Yangling 712100, China
Tel: +86-15584156891; E-mail: kuihl@jlu.edu.cn
DOI: https://doi.org/10.35633/inmateh-76-71

Keywords: *hazelnuts, discrete element, simulation parameter, calibration, repose angle*

ABSTRACT
To address the lack of contact parameters in designing hazelnut harvesting machinery, this study measured the physical properties of hazelnuts through experiments and obtained a 3D model via scanning. A DEM model was established accordingly. Contact parameters between hazelnuts and steel were calibrated through physical and simulated tests, yielding a restitution coefficient of 0.31, static friction of 0.39, and rolling friction of 0.04. Using the relative error of repose angle as the response variable and hazelnut–hazelnut contact parameters as factors, a quadratic regression model was developed by steepest ascent and Central Composite tests. The optimal contact parameters of hazelnuts were 0.11 (restitution), 0.21 (static friction), and 0.04 (rolling friction), with a 1.84% error.

摘要
为解决设计，优化榛子收获机械中缺乏接触参数的问题，本文通过试验测试得到了它的基本物理参数。通过 3D 技术得到了榛子的三维模型并建立了 DEM 模型。通过物理及模拟接触参数试验，测量及校准了榛子与钢的接触参数：恢复率 0.31，静摩擦率 0.39，滚动摩擦率 0.04。以物理与模拟堆积角的相对误差为响应值，以榛子间的接触参数为影响因子，通过最陡爬坡试验及中心组合试验建立二次回归模型，通过求解方程得到榛子间的最佳接触参数组合为：恢复系数 0.11，静摩擦系数 0.21，滚动摩擦系数 0.04，相对误差为 1.84%。

INTRODUCTION
Hazelnuts *(Corylus spp., family Betulaceae)* are among the world's four major nuts and serve as a vital oilseed crop. Their kernels are rich in essential amino acids, minerals, and unsaturated fatty acids that help lower blood lipids and support cardiovascular health *(Kruk et al., 2024; Bonisoil et al., 2015; Delprete et al., 2014)*. With recognized nutritional and medicinal value, hazelnuts are in growing demand globally. Rising health awareness and improved economic conditions have further boosted hazelnuts consumption. China is a leading producer, with output reaching 0.6 million tons in 2023 and showing steady annual growth *(Zhao et al., 2023; Guo et al., 2024)*.

The growing hazelnut market has driven the development of related machinery, with mechanization seen as a key solution to labor shortages intensified by China's aging population. However, equipment in this field remains in its early stages, lacking standardization and widespread adoption. To address terrain challenges, *Ren et al. (Ren et al., 2022; Ren et al., 2024)* developed a pneumatic harvester achieving a 96.332% picking rate with only 1.679% foreign material content. Further improvements enhanced operational stability. For shelling, *He et al., (2024),* proposed a conical sheller capable of processing hazelnuts of varying sizes, effectively improving shelling efficiency and reducing kernel breakage. The design and optimization of hazelnut-related machinery increasingly rely on computer-aided technologies such as DEM, CAE, and CAD, which streamline development and shorten design cycles. The Discrete Element Method (DEM), widely used in civil engineering, mining, and agricultural machinery, enables accurate simulation of granular material behavior. For example, *Zhang et al., (2024)*, developed a DEM model for alfalfa seeds, calibrating contact parameters via repose angle comparisons. Similarly, *Zhang et al., (2024),* established a safflower seed model using the Hertz–Mindlin (no slip) contact model and orthogonal testing. *Shi et al., (2024),* proposed a DEM model for cotton seeds, achieving accurate simulation of coated seed behavior for planting applications.

Mohammad et al., (2024), proposed a comprehensive five-step framework of a DEM grain model calibration and validation of flow and grain impacts on equipment was investigated. The flow model of corn during hopper unloading of the harvester was established and verified.

Currently, no studies have reported the development of a discrete element model (DEM) for hazelnuts or the calibration of their contact parameters, despite their importance for machinery design and optimization. In this study, the basic physical properties of hazelnuts were obtained through experimental measurement and theoretical calculation *(Sun et al., 2022)*. Contact parameters between hazelnuts and steel - including restitution, static friction, and rolling friction coefficients - were measured and calibrated using physical and simulated repose tests *(Wang et al., 2022; Xu et al, 2021, Xu et al., 2022)*. Using the relative error of repose angles as the response variable, and inter-hazelnut contact parameters as factors, the optimal parameter combination was identified through steepest ascent and the central composite tests *(Xu et al., 2018)*. Further validation confirmed the accuracy and reliability of the DEM model and calibrated parameters.

MATERIALS AND METHODS

Size Parameters

This study focuses on *Corylus avellana* (European hazelnut) as the target material. The hazelnut exhibits an approximately elliptical shape, with a nearly circular center that tapers toward both ends. Based on morphological features, the husk end is defined as the bottom and the pointed end as the top. During maturation, natural linear textures form along the husk surface. As shown in Figure 1, a three-dimensional rectangular coordinate system was established: the distance between the two vertices is defined as length (*L*), the axis along the husk's linear texture as width (*W*), and the axis perpendicular to it as thickness (*T*). A total of 200 hazelnuts were randomly selected for dimensional analysis. Using a digital caliper with 0.01 mm precision, the average values measured were 22.48 ± 0.96 mm (*L*), 18.23 ± 0.78 mm (*W*), and 17.46 ± 0.81 mm (*T*).

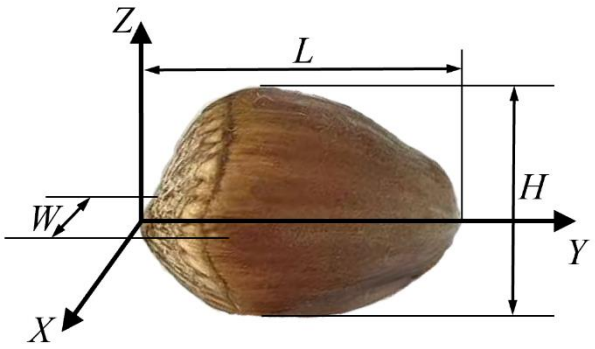

Fig. 1 – Schematic diagram of size characteristics of hazelnut

The density of hazelnuts

The mass of the hazelnuts was measured using an electronic balance with a precision of 0.01 g. Volume was determined via the liquid displacement method using a graduated cylinder (0.1 mL precision) filled with 99% ethanol. To minimize splashing and measurement error, the cylinder was tilted, and each hazelnut was gently introduced at the opening, allowing it to slide in slowly and become fully submerged. The hazelnut volume was calculated as the absolute difference between the initial and final liquid volumes. Ten hazelnuts were randomly selected, and the test was repeated five times per sample, with the average taken as the final result. Based on the standard formula for density *(Liu et al., 2025)*, the average density of hazelnuts was calculated to be 851 ± 15.37 kg/m³.

The Young's modulus and Poisson's ratio of hazelnuts

The Young's modulus is a measure of a material's ability to resist deformation under tension or compression and is one of the key mechanical properties of the hazelnut. The Young's modulus of the hazelnut was measured using a texture analyzer, as shown in Figure 2. The hazelnut was placed horizontally on the platform of the texture analyzer, and the hydraulic probe was manually adjusted to a suitable position above the hazelnut. The loading speed was set to 10 mm/s and pressure was applied until the breaking force in the dislocation-force curve in the computer reached its peak and decreased sharply, at which point the test was stopped.

The post-processing module of computer software was used to obtain the force-displacement curve during the seed compression test, as shown in Fig. 3(b). The indentation method is used to calculate the contact area, the surface of the hazelnut is coated with pigment, compressed to leave a near circular pattern on the hydraulic probe, and the contact area is calculated by the formula $A = \pi r^2$. The test was repeated seven times, and the average value was calculated. The Young's modulus of the hazelnut was then determined by Equation (1), yielding E = 1.254×10^9 Pa.

$$E = (\frac{\sigma}{A}) / v \tag{1}$$

where:

E is the Young's modulus of hazelnuts, Pa; σ represents the maximum compressive stress, Pa;

A represents the contact area of the compression head with the hazelnut, m^2; v is the line strain.

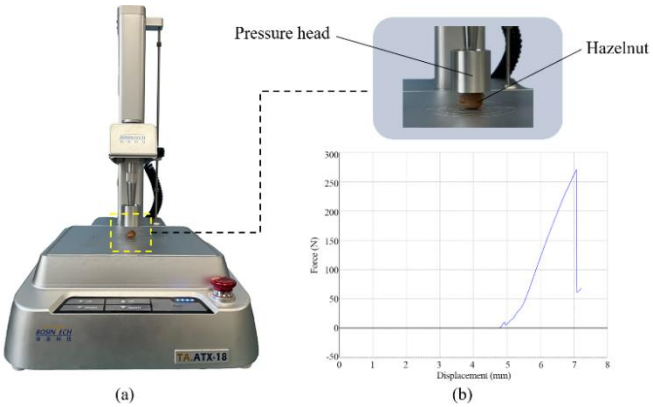

Fig. 2 – Hazelnuts mechanical properties test

(a) Hazelnuts compression test; (b) Load-displacement curve

Poisson's ratio is defined as the ratio of lateral strain to axial strain under uniaxial compression, and it is a key mechanical property of hazelnuts. In this study, a texture analyzer was used to perform compression deformation tests. Five hazelnuts were randomly selected, and their initial width and thickness were measured using a digital caliper. Each sample was placed on the test platform, and a hydraulic probe was manually positioned until it contacted the surface. The loading rate was set to 0.5 mm/s for a duration of 4 seconds. After compression, the width deformation was recorded. The test was repeated five times, and the average was used to calculate Poisson's ratio based on thickness and width changes. The resulting Poisson's ratio of hazelnuts was determined to be 0.38.

$$\lambda = \frac{\Delta T / T}{\Delta W / W} \tag{2}$$

where:

λ is Poisson's ratio of hazelnut; ΔT is the absolute deformation in the direction of the thickness of hazelnuts, mm; T is the original thickness of hazelnuts, mm; ΔW is the absolute deformation in the direction of the width of hazelnuts, mm; W is the original length in the direction of the width of hazelnuts, mm.

Discrete element method model

In this study, a three-dimensional model of a hazelnut was obtained using 3D scanning technology. A sample with dimensions close to the average was selected (Figure 3a), and its surface geometry was captured and smoothed using Materialise Magics 28.0 (Figure 3b). The processed model was exported in STL format and imported into EDEM 2022 (Figure 3c), where a discrete element model was generated using the automatic filling method (Figure 3d). This approach preserves the geometric fidelity and physical characteristics of the hazelnut, improving the accuracy and realism of simulation results for harvesting and processing applications. Contact interactions between hazelnuts and between hazelnuts and equipment surfaces were simulated using the Hertz–Mindlin (no slip) contact model. This model incorporates both elastic and frictional properties of materials, enabling accurate representation of collision and contact behaviors in the discrete element framework *(Li et al., 2024, Fan et al., 2021)*.

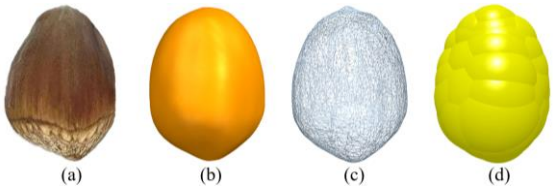

Fig. 3 – Hazelnut model

(a) Actual hazelnut; (b) Hazelnut scanning model, (c) Hazelnut profile model; (d) Hazelnut discrete element model

Determination and calibration of restitution coefficient

The collision restitution coefficient is defined as the ratio of separation velocity to approach velocity in the normal direction of contact and is influenced by the material properties of the colliding bodies. As illustrated in Fig. 4a, the restitution coefficient between hazelnuts and a steel plate was determined via a free-fall test. A hazelnut was released from a height of 500 mm above a horizontal steel surface, with vertical grid paper used for reference. The rebound motion was recorded using a high-speed camera, and the rebound height (h) was measured accordingly. This test was repeated ten times, yielding an average rebound height of 9.42 mm. The restitution coefficient was calculated using Equations 3–5, resulting in a value of 0.14 for the hazelnut–steel interaction.

$$e = \frac{v_4 - v_3}{v_2 - v_1} \tag{3}$$

$$v_4 = \sqrt{2gh} \tag{4}$$

$$v_2 = \sqrt{2gH} \tag{5}$$

where, e is the collision restitution coefficient between hazelnuts and steel; v_1 is the velocity of the steel before the collision, v_2 is the velocity of hazelnuts before the collision, mm·s^{-1}; v_3 is the velocity of the steel after the collision, mm·s^{-1}; v_4 is the velocity of hazelnuts after the collision, mm·s^{-1}; H is the height from which the object is dropped before free fall, mm; h is the rebound height, mm; g is the gravity acceleration, m·s^{-2}.

Due to deviations between physically measured and simulation-required restitution coefficients [30], calibration is necessary before applying values in DEM. As shown in Figure 4b, a simulation was conducted in EDEM 2022 under the same conditions as the physical free-fall test. The restitution coefficient ranged from 0.01 to 0.41 in steps of 0.05, while the static and rolling friction coefficients were fixed at measured values. Nine simulations were performed with a 5 s duration and a 0.001 s time step. A quadratic fit of the results is shown in Figure 5a. Substituting the physical rebound height (9.42 mm) into Equation (6) yielded a calibrated restitution coefficient of 0.31. This value was then verified through five repeated simulations, producing an average rebound height of 9.13 mm and a relative error of 3.08%. These results confirm that the calibrated coefficient closely reflects actual behavior and is suitable for further DEM simulations.

$$y_1 = 1.403 - 42.794x_1 + 217.095x_1^2 \tag{6}$$

where, x_1 is the restitution coefficient; y_1 is the rebound height, mm.

Determination and calibration of static friction coefficient

The static friction coefficient is defined as the ratio of the maximum static friction force to the normal force between two contact surfaces. It is influenced by material properties and surface roughness. In this study, the inclined plane method was used to measure the static friction coefficient between hazelnuts and a steel plate (Fig.4c). To prevent rolling, two hazelnuts were bonded together using adhesive. The inclined plane angle was gradually increased at a constant rate using a hand-cranked mechanism until the hazelnut assembly began to slide. The critical angle at the onset of sliding was recorded. This test was repeated 10 times, and the average value was calculated. The resulting average maximum static friction angle between the hazelnuts and the steel surface was 22.70°.

$$f = G\sin\theta \tag{7}$$

$$F_N = G\cos\theta \tag{8}$$

$$\mu = \frac{F_N}{f} \tag{9}$$

where: f is the frictional force acting on hazelnuts, N; G is the gravitational force on hazelnuts, N; F_N is the support force acting on hazelnuts, N; μ is the static friction coefficient; θ is the angle between the inclined plane and the horizontal surface, °.

The static friction coefficient was calculated using Equations (7)-(9), yielding a measured value of 0.42 for the hazelnut–steel interface. Calibration followed a similar procedure to that of the restitution coefficient. As shown in Figure 4d, a simulation of the inclined plane test was constructed in EDEM 2022 using the same initial and boundary conditions as the physical test. The restitution and rolling friction coefficients were fixed at previously determined values, while the static friction coefficient varied from 0.1 to 0.5 in 0.05 increments, requiring nine simulations. Each simulation lasted 15 s, with the plane rotating at 2°/s and a time step of 0.01s. The simulation results and quadratic fitting curve are shown in Figure 5b. Substituting the physical result (y_2 = 22.70°) into Equation (10), the calibrated static friction coefficient was determined to be 0.39. Repeated simulations yielded an average friction angle of 23.16°, with a relative error of 2.03%, confirming the calibration's accuracy.

$$y_2 = 0.944 + 59.548x_2 - 7.836x_2^{\,2} \tag{10}$$

where, x_2 is the static friction coefficient; y_2 is the maximum static friction angle,°.

Determination and calibration of rolling friction coefficient

Rolling friction refers to the resistance encountered when an object rolls over a surface without slipping, primarily caused by surface deformation at the contact interface. In this study, the bevel rolling method was used to determine the rolling friction coefficient between hazelnuts and a steel plate. As illustrated in Figure 4e, the inclined plane formed a 20° angle with the horizontal. Each hazelnut was placed at a distance of S = 150 mm from the incline's base and released from rest (initial velocity = 0 m/s). The hazelnut rolled freely until it came to a stop, and the horizontal rolling distance L was recorded. The test was repeated 10 times, and the average rolling distance was calculated to be 322.81 mm.

$$\mu' = \frac{GL\sin\beta}{G(L\cos\beta + S)} \tag{11}$$

where, G is the gravitational force on the hazelnut, N; β is the angle of inclination of the inclined plane, °; S is the distance traveled by the hazelnut while rolling on a flat surface, mm; L is the distance traveled by the hazelnut while rolling on an inclined plane, mm; μ' is the rolling friction coefficient of the hazelnut and steel plate.

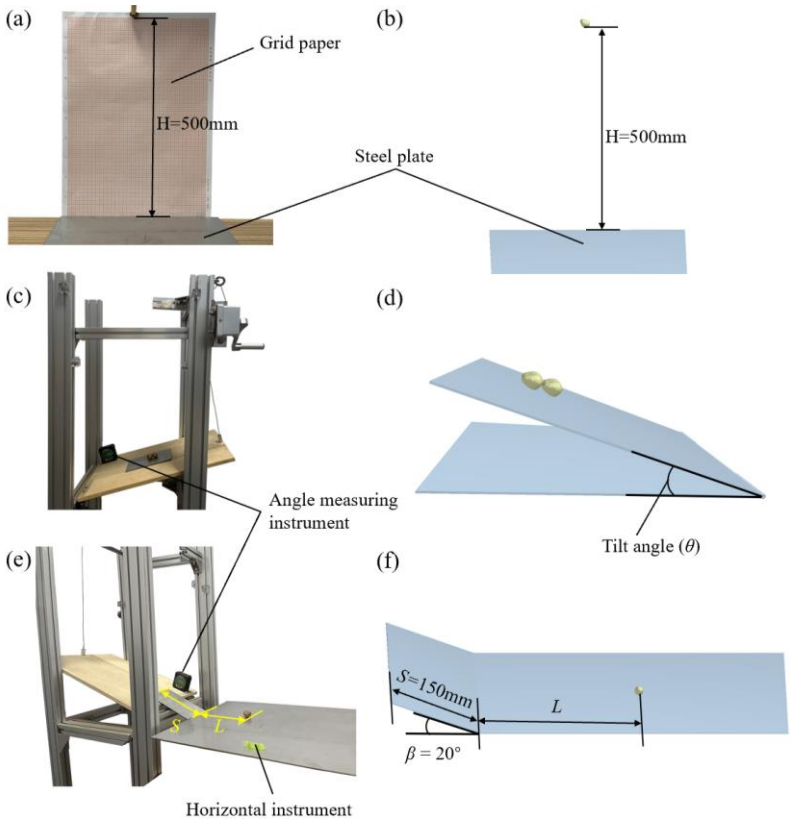

Fig. 4 - Physical test and simulated test for measuring contact parameters of hazelnuts and steel

(a) Physical collision test; (b) Simulated collision test; (c) Physical static friction coefficient test; (d) Simulated static friction coefficient test; (e) Physical rolling friction coefficient test; (f) Simulated rolling friction coefficient test.

The rolling friction coefficient is calculated using Equation (11). The rolling friction coefficient between hazelnuts and the steel plate is calculated to be 0.11.

A simulation test replicating the physical rolling friction experiment was constructed in EDEM 2022, as shown in Figure 4f. The restitution and static friction coefficients were fixed at their calibrated values. The rolling friction coefficient was varied from 0.01 to 0.17 in 0.02 increments, resulting in nine simulations. The simulation results and the corresponding quadratic fitting curve are presented in Figure 5c. By substituting the physical rolling distance (y_3 = 322.81 mm) into Equation (12), the calibrated rolling friction coefficient was determined to be 0.04. This value was then applied in a second round of simulations (n = 10), producing an average rolling distance of 313.46 mm. The relative error between the physical and simulated results was 2.90%, confirming that the calibrated rolling friction coefficient closely reflects actual behavior and is reliable for subsequent discrete element simulations.

$$y_3 = 345.71 - 680.14x_3 + 2059.71{x_3}^2 \quad (12)$$

where, x_3 is the rolling friction coefficient; y_3 is the rolling distance, mm.

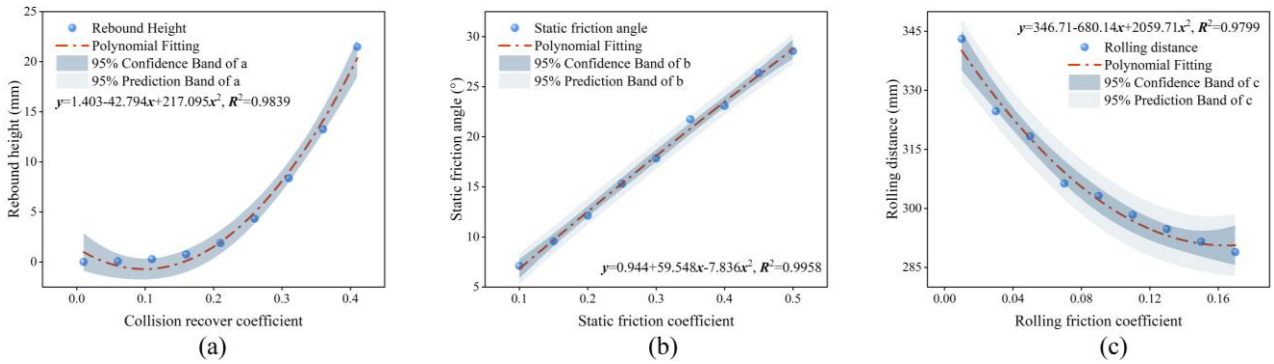

Fig. 5 - Simulation results of hazelnut and steel contact parameters and polynomial fitting

(a) Simulation results of restitution coefficient test and quadratic fitting; (b) Simulation results of static friction coefficient test and quadratic fitting; (c) Simulation results of rolling friction coefficient test and quadratic fitting.

Calibration of contact parameters between hazelnuts

Direct measurement of contact parameters between hazelnuts using conventional methods is challenging. Therefore, this study employs a combined approach of physical and simulated repose angle tests for calibration. The relative error between physical and simulated repose angles serves as the response variable, while the restitution coefficient, static friction coefficient, and rolling friction coefficient between hazelnuts are treated as experimental factors. Using steepest ascent and orthogonal test methods, a regression model is established, and the optimal combination of inter-hazelnut contact parameters is determined for accurate discrete element simulation *(Ucgul et al., 2018, Gu et al. 2020)*.

Physical repose test

The physical repose angle tests were conducted using the cylindrical lifting method. The test apparatus comprised a steel cylinder (100 mm diameter, 400 mm height) and a steel plate (400 × 400 mm, 2 mm thick). Before testing, the cylinder was placed at the center of the plate and filled with hazelnuts. It was then lifted vertically at a constant speed of 30 mm/s, allowing the hazelnuts to form a natural pile, as shown in Figure 6a. Image processing was performed in MATLAB, including binarization, hole filling (Figure 6b), edge extraction, and linear fitting using the least squares method to determine the slope on both sides of the pile (Figures 6c and 6d). Due to asymmetry, the average of the absolute values of both side slopes was taken as the repose angle for each test. The procedure was repeated 10 times, yielding an average repose angle of 23.38 ± 0.72°.

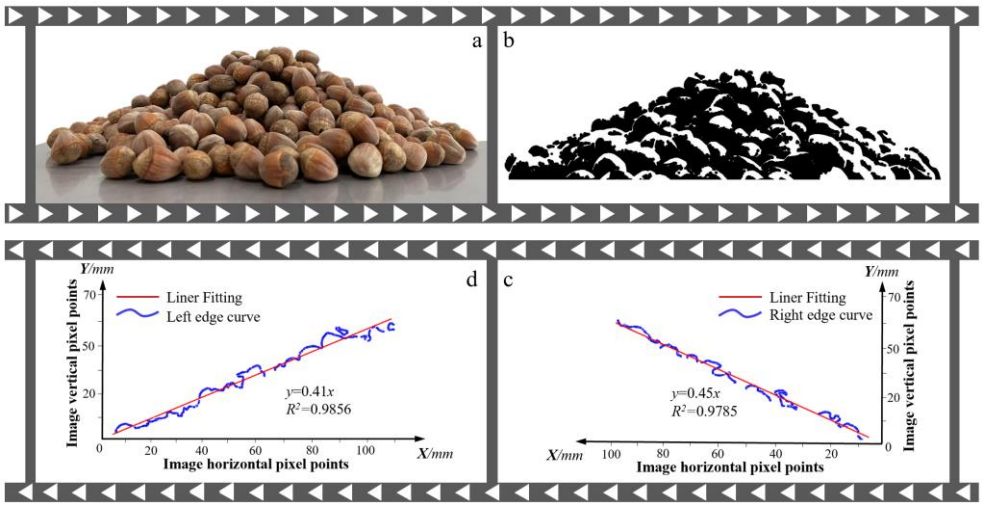

Fig. 6 - Physical repose tests and experimental processing.

(a) Physical angle of repose test; (b) Using MATLAB to process the figures; (c) Right side repose curve; (d) Left side repose curve.

Simulation repose test

A simulated repose angle test replicating the physical test was established in EDEM 2022, as shown in Figure 7a. Contact parameters between hazelnuts and the steel tube/plate were set according to values listed in Table 2. The lifting direction of the steel tube was aligned with the positive z-axis, at a velocity of 0.03 m/s. The total simulation time was set to 8 s, with a data-saving interval of 0.1 s, as only the final repose state was of interest. The simulation process and resulting particle pile formation are illustrated in Figures 7b–7d. For analysis, the post-processing view was set to the XZ plane, and particle color was rendered black. The final pile shape was processed using MATLAB, where edge detection and least squares fitting were performed to extract the slope values, as shown in Figure 7e.

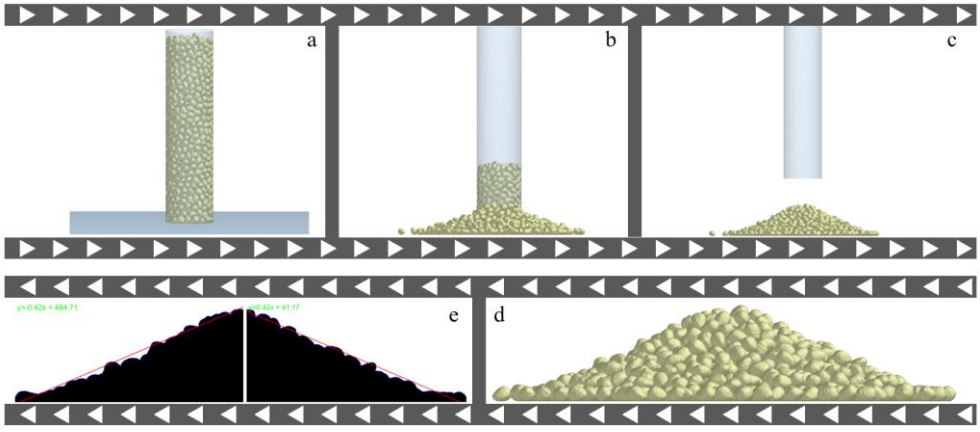

Fig. 7 - Simulated Repose Tests and Experimental Processing.

(a) Before simulated tests; (b) During simulated tests; (c) After simulated tests; (d) Hazelnuts stacking; (e) Repose angle measurement

The steepest climb test

The steepest ascent method was employed to quickly approach the optimal range of these significant factors. The experimental design is shown in Table 1.

Table 1

Design of the steepest climb test

NO.	Test factors		
	X_1	X_2	X_3
1	0.1	0.1	0.01
2	0.2	0.2	0.02
3	0.3	0.3	0.03
4	0.4	0.4	0.04
5	0.5	0.5	0.05

Central composite design with quadratic orthogonal rotations

Based on the optimal factor ranges determined from the steepest ascent test, three levels of restitution coefficient, static friction coefficient, and rolling friction coefficient were selected for a central composite design with quadratic orthogonal rotation. A response surface model was then established using the experimental results, and a regression equation was derived. This equation was used to predict the optimal combination of contact parameters between hazelnuts that best approximates the actual repose angle, enabling improved accuracy in the discrete element simulation.

RESULTS

Results of the steepest climb test

The results of the steepest ascent test are presented in Figure 8. As the restitution coefficient, static friction coefficient, and rolling friction coefficient increased, the relative error between simulated and physical repose angles initially decreased and then increased. Test Group No. 2 produced the lowest relative error of 2.61% and was therefore selected as the zero level for the subsequent response surface design. The optimal range of factor levels was determined to lie between those of Group No. 1 and Group No. 3, providing the basis for refined parameter optimization.

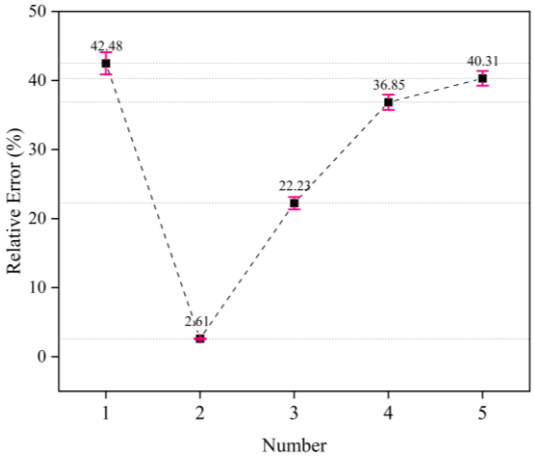

Fig. 8 – Results of the steepest climb test

Results of the quadratic orthogonal rotating combination test

The results and analysis of variance for the three-factor, five-level orthogonal rotating combination test are presented in Table 2 and Table 3.

Table 2

Test result of the central composite test

No.	X_1	X_2	X_3	Relative Error (Y)
1	-1	-1	-1	48.10
2	1	-1	-1	51.65
3	-1	1	-1	3.63
4	1	1	-1	3.55
5	-1	-1	1	24.16
6	1	-1	1	20.78
7	-1	1	1	1.54
8	1	1	1	19.37
9	-1.682	0	0	2.52
10	1.682	0	0	0.51
11	0	-1.682	0	64.73
12	0	1.682	0	0.51
13	0	0	-1.682	26.38
14	0	0	1.682	19.37
15	0	0	0	0.51
16	0	0	0	11.03
17	0	0	0	0.51
18	0	0	0	2.61
19	0	0	0	0.56
20	0	0	0	0.51

The data in Table 4 were analyzed using Design-Expert 13.0. A regression model was established to describe the relative error of repose angle as a function of the restitution coefficient (X_1), static friction coefficient (X_2), and rolling friction coefficient (X_3) between hazelnuts. The fitted regression equation is shown in Equation (13).

$$Y = 2.57 + 1.06X_1 - 16.45X_2 - 3.87X_3 + 2.20X_1X_2 + 1.37X_1X_3 + 8.57X_2X_3 - 0.05X_1^2 + 10.94X_2^2 + 7.50X_3^2 \quad (13)$$

The ANOVA results for the regression model (Equation 13) are summarized in Table 5. A P-value < 0.0001 indicates the model is highly significant, while the lack of fit (P = 0.1813) is not significant, confirming the model's adequacy. The coefficient of determination (R^2) is 0.9586, indicating strong predictive reliability. Among the factors, the static friction coefficient (X_2) has a highly significant effect, followed by the rolling friction coefficient (X_3), while the restitution coefficient (X_1) shows no significant impact. Only the interaction between X_2X_3 is statistically significant. The response surface of X_2X_3 (Figure 10) shows that as both static and rolling friction coefficients increase, the relative error first decreases and then rises. The steeper, denser contours of X_2 indicate its greater influence, consistent with the ANOVA findings. The factors affecting repose angle error, in order of significance, are X_2, X_3, and X_1 *(Zhuang et al, 2023)*.

Table 3

ANOVA for quadratic equation model

Parameters	Sum of Squares	Df	Mean square	F value	P value
Modal	6922.69	9	769.19	25.74	<0.0001**
X_1	15.48	1	15.48	0.5181	0.4882
X_2	3693.92	1	3693.92	123.63	<0.0001**
X_3	204.67	1	204.67	6.85	0.0257*
X_1X_2	38.63	1	38.63	1.29	0.2820
X_1X_3	15.07	1	15.07	0.5044	0.4938
X_2X_3	587.22	1	587.22	19.65	0.0013**
X_1^2	0.0413	1	0.0413	0.0014	0.9711
X_2^2	1725.98	1	1725.98	57.76	<0.0001*
X_3^2	810.28	1	810.28	27.12	0.0004**
Residual	298.79	10	29.88		
Lack of Fit	210.47	5	42.09	2.38	0.1813
Pure Error	88.33	5	17.67		
Cor Total	7221.49	19			

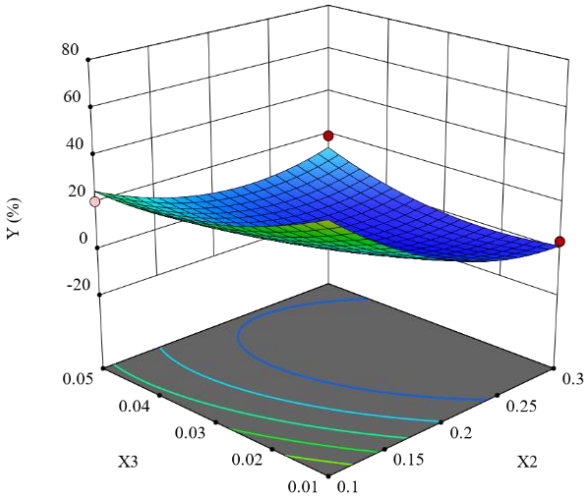

Fig. 10 - Effect of static friction coefficient and rolling friction coefficient on the relative error

Parameter optimization

Based on the experimental data and regression equation, the optimization module in Design-Expert 13.0 was used to minimize the relative error (Y). The software identified the optimal combination of significant factors that resulted in the lowest predicted error, providing the best-fit contact parameters for accurate repose angle simulation.

The objective function and constraints are as following equation (14):

$$\begin{cases} \min Y(X_1, X_2, X_3) \\ \begin{cases} 0.1 \le X_1 \le 0.3 \\ 0.1 \le X_2 \le 0.3 \\ 0.01 \le X_3 \le 0.05 \end{cases} \end{cases} \quad (14)$$

The optimized contact parameters between hazelnuts were: restitution coefficient 0.11, static friction coefficient 0.21, and rolling friction coefficient 0.04. These values were applied in EDEM, and 10 simulated repose angle trials were conducted. The average simulated repose angle was 23.82°, with a relative error of only 1.84 ± 0.009%. This confirms that the optimized parameter set is highly accurate and suitable for use in subsequent discrete element simulations.

CONCLUSIONS

1. The fundamental physical properties of hazelnuts—including size, density, Young's modulus, and Poisson's ratio—were measured through physical testing. Contact parameters between hazelnuts and steel were obtained and calibrated using a combination of experiments and simulations. A 3D model was built via scanning, and a DEM model was generated using the automatic filling method. The calibrated parameters were: restitution coefficient 0.31, static friction 0.39, and rolling friction 0.04.

2. Contact parameters between hazelnuts were calibrated using combined physical and simulated repose tests. Image analysis in MATLAB enabled accurate measurement of the repose angle. A steepest ascent test identified optimal parameter ranges, followed by response surface optimization. The final calibrated values were 0.11 (restitution), 0.21 (static friction), and 0.04 (rolling friction), yielding a relative error of 1.84 ± 0.009% in validation tests—demonstrating high model accuracy.

3. The calibrated contact parameters provide a reliable foundation for DEM-based design and optimization of hazelnut harvesting, handling, and cleaning machinery, helping reduce development costs and improve efficiency.

ACKNOWLEDGEMENT

This work was supported financially by the Natural Science Foundation of Jilin Province (No. 0250102113JC)

REFERENCES

[1] Bonisoil, E.; Delprete, C.; Sesana, R.; Tamburro, A.; Tornincasa, S. (2015). Testing and Simulation of the three point bending anisotropic behaviour of hazelnut shells. *Biosyst. Eng.,* Vol.129, pp: 134–141;

[2] Chen, X. Y., Wang, X. Z., Bai, J., Fang, W. Q., Hong, T. Y., Zang, N., Wang, G. L. (2024). Virtual parameter calibration of pod pepper seeds based on discrete element simulation. *Heliyon*, Vol.10, Issue 11, e31686

[3] Delprete, C.; Sesana, R. (2014). Mechanical characterization of kernel and shell of hazelnuts: Proposal of an experimental procedure. *J. Food Eng.*, Vol.124, pp: 28–34;

[4] Fan, R., Cui, Q. L., Zhang, Y. Q., Lu, Q. (2021). Analysis and calibration of parameters of buckwheat grain based on the repose experiment. *INMATEH-Agricultural Engineering*, Vol.64, Issue 2, pp: 467-476

[5] Gu, Z. Y., Cao, M. C. (2024). Analysis of unstable block by discrete element method during blasting excavation of fractured rock mass in underground mine. *Heliyon,* Vol.9, Issue 11, e22558

[6] Guo, Y., Chen, Q. S., Xia, Y. D., Westover, T., Eksioglu, S., Roni, M. (2020). Discrete element modeling of switchgrass particles under compression and rotational shear. *Biomass and Bioenergy*, Vol.141, 105649

[7] He, T., Liu, K., Zhang, R., Ren, G. Y., Liu, Z. H., (2024). Development of high efficiency hazelnut shell breaking machine. *Food & Machinery*, Vol. 40, Issue 5, pp: 88-95;

[8] Kruk, M., Ponder, A., Horoszewicz, J., Poplawski, D., Krol, K., Leszczynska, J., Jaworska, D., Trzaskowska, M. (2024). By-product hazelnut seed skin characteristics and properties in terms of use in food processing and human nutrition. *Scientific Reports*, Vol.14, Issue 1, 18835;

[9] Liu, J., Lu, T., Zheng, S., Tian, Y., Han, M., Tai, M., He, X., Li, H., Wang, D., Zhao, Z. (2025). Parameter Calibration Method for Discrete Element Simulation of Soil-Wheat Crop Residues in Saline-Alkali Coastal Land. *Agriculture*, Vol.15, Issue 2, 129;

[10] Li, Y. F., Zhou, W. Q., Ma, C. C., Feng, Z. H., Wang, J. W., Yi, S. J., Wang, S. (2024). Design and optimization of the seed conveying system for belt-type highspeed corn seed guiding device. *International Journal of Agricultural and Biological Engineering*, Vol.17, Issue 02, pp: 123-131;
[11] Mohammad, M., Mehari Z.T. (2024). Systematic Calibration and Validation Approach for Discrete element Method (DEM) Modeling of Corn under Varying Moisture Contents (MC). *J. ASABE*, Vol.67, Issue 2, pp: 259-274;
[12] Ren, D. Z., Yu, H. L., Zhang, R., Li, J. Q., Zhao, Y. B., Liu, F. B., Zhang, J. H., Wang, W. (2024). Topology Optimization Design and Modal Analysis of Hazelnut Picking and Sorting Machine. *Journal of Agricultural Mechanization Research*, Vol.46, Issue 05, pp: 19-25;
[13] Ren, D. Z., Yu, H. L., Zhang, R., Li, J. Q., Zhao, Y. B., Liu, F. B., Zhang, J. H., Wang, W. (2022). Research and experiments of hazelnut harvesting machine based on CFD-DEM analysis. *Agriculture*, Vol.12, Issue 12, 2115;
[14] Sun, K., Yu, J. Q., Liang, L. S., Wang, Y., Yan, D. X., Zhou, L., Yu, Y. J. (2022). A DEM-based general modelling method and experimental verification for wheat seeds. *Powder Technology*, Vol. 401, 117353;
[15] Ucgul, M., Saunders, C., Fielke, J. M. (2018). Comparison of the discrete element and finite element methods to model the interaction of soil and tool cutting edge. *Biosystems Engineering*, Vol.169, pp: 199-208;
[16] Wang, S., Yu, Z. H., Aorigele, Zhang, W. J. (2022). Study on the modeling method of sunflower seed particles based on the discrete element method. *Computers and Electronics in Agriculture*, Vol.198, 107012;
[17] Xu, B., Zhang, Y. Q., Cui, Q. L., Ye, S. B., Zhao, F. (2021). Construction of a discrete element model of buckwheat seeds and calibration of parameters. *INMATEH-Agricultural Engineering*, Vol.64, Issue 02, pp: 175-184;
[18] Xu, B., Zheng, D. C., Cui, Q. L. (2022). Experimental research on three-level vibrating screening of buckwheat based on discrete element method. *INMATEH-Agricultural Engineering*, Vol.68, Issue 03, pp: 191-200;
[19] Xu, T. Y., Yu, J. Q., Yu, Y. J., Wang, Y. (2018). A modelling and verification approach for soybean seed particles using the discrete element method. *Advanced Powder Technology*, Vol.29, Issue 12, pp: 3274-3290;
[20] Zhao, J. R., Wang, X. H., Lin, H., Lin, Z. (2023). A comprehensive review of nutrition, phytochemical profile, extraction, bioactivities and applications. *Food Chemistry*, Vol.413, 135576;
[21] Zhang, X. J., Wang, H. T., Wang, F. Y., Lian, Z. G. (2024). Parameter calibration of discrete element model for alfalfa seeds based on EDEM simulation experiments. *International Journal of Agricultural and Biological Engineering*, Vol.17, Issue 3, pp: 33-38;
[22] Zhang, Z. G., Zeng, C., Xing, Z. Y., Xu, P., Guo, Q. F., Shi, R. M., Wang, Y. Z. (2024). Discrete element modeling and parameter calibration of safflower biomechanical properties. *International Journal of Agricultural and Biological Engineering*, Vol.17, Issue 2, pp: 37-46;
[23] Zhuang, H. Y., Wang, X. L., Zhang, X. C., Cheng, X. P., Wei, Z. C. (2023). Discrete element-based design of key parameters for wheel rut tillage devices. *Engenharia Agricola*, Vol.43, Issue 3, e20230039;
[24] Zhao, J. W., Yu, J. Q., Sun, K., Wang, Y., Liang, L. S., Sun, Y. C., Zhou, L., Yu, Y. J. (2024). A discrete element method model and experimental verification for wheat root systems. *Biosystems Engineering*, Vol.244, pp: 146-165.